

RESEARCH

Open Access



LincRNA-ASAO promotes dental pulp repair through interacting with PTBP1 to increase ALPL alternative splicing

Fuchun Fang^{1†}, Xiaolan Guo^{2,3†}, Sitong Liu¹, Longrui Dang¹, Zehao Chen¹, Yumeng Yang¹, Lu Chen¹, Jiahao Lin¹, Wei Qiu^{1*}, Zhao Chen^{1,2*} and Buling Wu^{1,2,3*} 

Abstract

Background Alternative splicing not only expands the genetic encoding of genes but also determines cellular activities. This study aimed to elucidate the regulation mechanism and biological functions of lincRNA-ASAO in the process of odontogenesis-related genes alternative splicing mediated odontogenic differentiation of hDPSCs.

Methods RACE, RNA-seq, FISH and bioinformatics techniques were used to identify novel lincRNA-ASAO. ALP staining, alizarin red staining, qRT-PCR and western blot were used to identify the role of lincRNA-ASAO in regulating the odontoblast differentiation of hDPSCs. The binding protein PTBP1 of lincRNA-ASAO was screened by RNA-Pull-down, protein profiling and bioinformatics. The target gene ALPL of lincRNA-ASAO/PTBP1 was identified by RNA-seq, bioinformatics technology and DNA agarose gel electrophoresis. FISH, IF, PAR-CLIP and bioinformatics techniques were used to determine the roles of lincRNA-ASAO, PTBP1 and ALPL pre-mRNA in the odontoblast differentiation of hDPSCs.

Results We identified a novel lincRNA-ASAO that could promote the odontogenic differentiation of human Dental Pulp Stem Cells (hDPSCs). And, the interaction between lincRNA-ASAO and alternative splicing factor PTBP1 promoted the odontoblast differentiation of hDPSCs. In addition, lincRNA-ASAO forms duplexes with ALPL pre-mRNA, targeting PTBP1 to exonic splicing silencer (ESS) of ALPL and regulating exon 2 skipping. Notably, lincRNA-ASAO/PTBP1 regulated ALPL production to increase the type 2 splice variant, which promoted the odontoblast differentiation of hDPSCs.

Conclusions We have identified the novel lincRNA-ASAO, which can promote the odontoblast differentiation of hDPSCs. The mechanism study found that lincRNA-ASAO/PTBP1 mediated the exon 2 skipping of ALPL pre-mRNA, resulting in the type 2 splice variant of ALPL. Our results enrich the understanding of lncRNAs and alternative splicing in regulating the odontoblast differentiation of hDPSCs, and provide clues to improve the clinical therapeutic potential of hDPSCs for dental pulp restoration.

Keywords Odontogenesis, PTBP1, hDPSCs, lncRNA, Alternative splicing

[†]Fuchun Fang and Xiaolan Guo have contributed equally to this work.

*Correspondence:

Wei Qiu

Zhao Chen

Buling Wu

bulingwu@smu.edu.cn

Full list of author information is available at the end of the article



© The Author(s) 2025. **Open Access** This article is licensed under a Creative Commons Attribution-NonCommercial-NoDerivatives 4.0 International License, which permits any non-commercial use, sharing, distribution and reproduction in any medium or format, as long as you give appropriate credit to the original author(s) and the source, provide a link to the Creative Commons licence, and indicate if you modified the licensed material. You do not have permission under this licence to share adapted material derived from this article or parts of it. The images or other third party material in this article are included in the article's Creative Commons licence, unless indicated otherwise in a credit line to the material. If material is not included in the article's Creative Commons licence and your intended use is not permitted by statutory regulation or exceeds the permitted use, you will need to obtain permission directly from the copyright holder. To view a copy of this licence, visit <http://creativecommons.org/licenses/by-nc-nd/4.0/>.

Background

Eukaryotic genes consist of a combination of exons and introns, and alternative splicing at various sites expands the coding capacity of eukaryotic genes [1]. Peptides generated from a single gene through alternative splicing are often similar but not identical, leading to subtle or significant variations at the mRNA and protein levels [2, 3]. More than 95% of human exonic genes undergo alternative splicing, which is tightly controlled by the interaction between post-transcriptionally acting proteins known as splicing factors and cis-acting nucleotide sequences [4, 5]. These splicing factors encompass members of the heterogeneous nuclear ribonucleoprotein (hnRNP) family, which either promote or inhibit specific splicing events by interacting with exonic or intronic regulatory sequences categorized as enhancers or silencers [6–9]. Alternative splicing events play a regulatory role in a wide array of cellular biological processes, influencing cell differentiation, proliferation, and apoptosis [10–13].

Stem cells hold immense potential for treating various human diseases and conditions. The process of stem cell differentiation produces multiple transcripts through alternative splicing, generating tissue-specific mRNA and protein isoforms that serve as key regulators of gene expression [14, 15]. Early genome-wide analyses have revealed more than 1000 genes with alternative splicing events in stem cells [16]. Using alternative splicing microarrays, researchers have identified altered splicing patterns in 170 of 40,000 putative exon-exon junctions in embryonic stem cells (ESCs), with 67% of these events predicted to alter protein sequence and domain composition [17]. In recent years, with the successful isolation and culture of hDPSCs, an increasing number of studies have confirmed their important role in pulp injury repair, particularly through differentiation into various cell types to promote pulp tissue regeneration [18]. hDPSCs can differentiate into odontoblast-like cells, forming dentin-like hard tissue in the injured pulp area, which helps repair dentin defects [19]. Additionally, they can differentiate into endothelial cells, promoting angiogenesis to improve local blood supply, providing sufficient nutrients and oxygen to support tissue regeneration and repair [20]. On the other hand, hDPSCs can also differentiate into neural cells, helping to restore neural function in the damaged area, alleviate pain, and promote nerve tissue recovery [19]. Through the differentiation of these cells, hDPSCs effectively promote pulp tissue regeneration and functional recovery, enhancing the repair capacity after injury.

hDPSCs are seed cells for pulp repair, and some studies focus on the potential role of alternative splicing events in hDPSCs during pulp repair. The inclusion of exon 5

in RUNX2 is critical for maintaining the transcriptional activity of RUNX2. The splicing factor YBX1 promotes the inclusion of RUNX2 exon 5, enhancing the mineralization ability of DPSCs [21]. However, hnRNP A1 has an opposite effect compared to YBX1 in regulating RUNX2 exon 5 inclusion and odontogenic differentiation of hDPSCs. hnRNP A1 inhibits the inclusion of RUNX2 exon 5, thereby suppressing odontoblastic differentiation [22]. Additionally, N6-adenosine methyltransferase 3 mediates the expression of the MyD88S variant, which inhibits inflammation and can partially suppress LPS-induced DPC inflammatory responses, playing a protective role in pulp inflammation [23]. These studies suggest that splice variants may have a potential role in pulp repair. However, research on the regulation of gene-specific splicing in hDPSC differentiation and its application in pulp repair is still relatively limited, and its mechanisms and clinical applications require further exploration.

Long non-coding RNAs (lncRNAs), characterized by lengths of more than 200 non-protein coding nucleotides, represent the largest subclass of non-coding RNAs [18, 24]. Extensive research over the past decade has revealed that lncRNAs are involved in the regulation of cell differentiation through their participation in alternative splicing [25, 26]. For instance, the lncRNA TOBF1 governs the fate of mouse ESCs by modulating the alternative splicing of pluripotency genes [27]. Another study investigated the interaction between the lncRNA Protein Phosphatase 2A Regulatory Subunit A Beta Isoform (PPP2R1B) and hnRNPLL, which promotes osteogenic differentiation of mesenchymal stem cells (MSCs) by regulating the alternative splicing of PPP2R1B [28]. In addition, the lncRNA Pnky and PTBP1 have been found to facilitate the differentiation of neural stem cells by regulating the alternative splicing of a core set of transcripts associated with cell phenotype [26].

However, whether lncRNAs play a role in regulating alternative splicing events in hDPSCs during dental pulp repair remains an unanswered question. Initially, we conducted a transcriptome analysis to identify lncRNAs that are differentially expressed in DPSCs after odontoblast induction [29]. After applying strict conditions, the only highly expressed lncRNA G018548 was selected. And we identify G018548 as an alternative splicing-associated odontoblastic differentiation lncRNA (named lincRNA-ASAO) that contributes to dental pulp repair. The primary objective of this study was to elucidate the potential role of lincRNA-ASAO in dental pulp regeneration and to uncover the underlying molecular mechanisms driving reparative dentin formation.

Methods

Patients and tissue collection

Dental pulp tissue samples were obtained from third molars extracted from 18–24-year-old patients at the Department of Stomatology. All experimental protocols were approved by Medical Ethics committee of Nan-Fang Hospital of Southern Medical University (NFEC-202302-K5-01). A total of 10 healthy tooth samples and 10 carious tooth samples were collected for the subsequent experiment. The patient information is presented in Table 1. The exclusion criteria included hematologic disorders, cardiovascular and respiratory diseases, diabetes, systemic inflammation or non-plaque-induced oral inflammation, immunosuppressive chemotherapy, and current pregnancy or lactation.

Isolation of primary hDPSCs

Dental pulp tissue samples were obtained from third molars extracted from 18–24-year-old patients at the Department of Stomatology of NanFang Hospital of Southern Medical University. All experimental protocols were approved by Medical Ethics committee of Nan-Fang Hospital of Southern Medical University (NFEC-202302-K5-01). The collected dental pulp tissues were then cut into 1–2 mm tissue blocks and incubated with 1 mg/ml type I collagenase (C8140-100, solarbio) for 15 min. The tissue blocks were placed in cell culture flasks for cultivation, and the isolated cells were identified. The

isolated hDPSCs were cultured in Dulbecco’s Modified Eagle Medium (DMEM) supplemented with 10% fetal bovine serum (FBS) (Gibco, Grand Island, NY, USA) and 100 U/mL penicillin/streptomycin (HyClone, NY, USA), and maintained at 37 °C in a humidified atmosphere containing 95% air and 5% CO₂. Cells were filtered through a 70 µm filter (BD Falcon, Franklin Lakes, NJ) to obtain a single-cell suspension. The single-cell suspension was seeded at a density of 1×10⁴ cells/well in a 6-well plate. Single-cell-derived colonies were obtained using limiting dilution technique. The cells were identified by flow cytometry (Becton Dickinson, Tokyo, Japan) using stem cell surface markers (CD44, CD90, CD45, CD34). The specific methods followed the previous research [29].

Odontogenic induction

In the differentiated group, hDPSCs were cultured in odontogenic differentiation medium containing 50 mg/mL ascorbic acid (255564-100G, Sigma-Aldrich), 100 nmol/L dexamethasone (D4902, Sigma-Aldrich), and 10 mmol/L β-glycerophosphate (G9422, Sigma-Aldrich) for 14 days in 6-well plates. hDPSCs in the undifferentiated group were cultured in DMEM with 10% FBS and no additional supplements. Samples can be collected for subsequent experiments and analysis after 14 days of odontogenic differentiation induction of hDPSCs. The specific methods followed the previous research [29].

Rapid-amplification of cDNA ends (RACE)

To obtain the full-length cDNA sequence, the RACE 5’/3’ Kit (Takara, 634858) was used for RACE. In brief, 1 µg of freshly isolated RNA from hDPSCs was used to generate the first-strand cDNA according to the experimental steps. The primer design was performed with Tm between 60 °C and 70 °C. The polymerase chain reaction (PCR) products were used for nested PCR to verify the 5’ and 3’ ends. The PCR products were extracted and purified from agarose gels before sequencing. After obtaining the full-length sequence, RNA samples from hDPSCs were collected and PCR was performed using four specific primers. The PCR products were separated by 1% agarose gel electrophoresis.

Lentivirus transduction

The overexpression plasmids of lincRNA-ASAO, Polypyrimidine Tract Binding Protein 1 (PTBP1 or hnRNPI), and the negative control group were designed and constructed by OBiO Technology (Shanghai, China). The vector components used for overexpressing lincRNA-ASAO included pASLenti-pA-MCS-CMV-EF1-mCherry-P2A-BSR-WPRE, while those used for overexpressing PTBP1 included pSLenti-SFH-EGFP-P2A-Puro-CMV-3xFLAG-WPRE. According to the manufacturer’s instructions,

Table 1 Participant details

	Age	Gender	Tooth site
Healthy pulp	23	Female	18
	23	Female	28
	22	Female	28
	19	Female	48
	18	Female	28
	21	Male	18, 28
	20	Male	18, 28
	19	Male	38, 48
	21	Male	18, 28
	23	Male	28, 38
Carried pulp	22	Female	18
	22	Female	28
	24	Female	28
	22	Male	48
	18	Male	38
	19	Male	18, 28
	18	Male	38, 48
	20	Female	18, 48
	21	Female	18, 28
	21	Male	38, 48

hDPSCs at passages 3–5 were seeded in cell culture flasks and transfected with the corresponding lentiviral vectors to generate stable cell lines for subsequent experiments. The transfection efficiency was validated by quantitative real-time quantitative PCR (qRT–PCR) and western blotting.

Short hairpin RNA (shRNA) oligos

The lincRNA-ASAO, PTBP1, and negative control group shRNA lentiviral vectors were designed and constructed by Genewell Company (Shenzhen, China). The vector components used for inhibiting lincRNA-ASAO included pCLenti-U6-shRNA-CMV-EGFP-F2A-BSR-WPRE, while those used to inhibit PTBP1 included pCLenti-U6-shRNA-CMV-mCherry-F2A-Neo-WPRE. The 3rd–5th generation hDPSCs were seeded in T25 flasks, transduced with the virus, and established as stable cell lines for subsequent experiments. The transfection efficiency was validated using qRT–PCR and western blotting.

RNA extraction and reverse transcription

The total RNA was extracted from the dental pulp tissue or hDPSCs using TRIzol reagent (Invitrogen, Life Technologies) according to the manufacturer’s protocol. The concentration and quality of RNA were measured using a NanoDrop ND-2000 spectrophotometer (ThermoFisher Scientific, Waltham, MA, USA). For cDNA synthesis, 1000 ng of total RNA was reverse transcribed using the PrimeScript RT Kit (TaKaRa, Shiga, Japan) according to the manufacturer’s instructions.

qRT–PCR

According to the manufacturer’s instructions, total RNA was extracted from tissues using the EZ-press RNA Purification Kit (ezbioscience, USA) and quantified using the NanoDrop ND-1000 spectrophotometer (Thermo Scientific, USA). qRT–PCR was performed on a Roche Light-Cycler®480 using the Color SYBR Green qPCR Master Mix ROX2 (ezbioscience, USA). Each reaction contained 5 µL of 2×Color Green qPCR Master Mix, 0.2 µL of forward primer, 0.2 µL of reverse primer, 2.6 µL of RNase Free ddH₂O, and 2 µL of reverse transcription product. The relative gene expression level was calculated using the 2-ΔΔCt method, and all experiments were repeated three times. The gene-specific primer sequences are listed in Table 2.

Western blotting

Cellular total protein was extracted using protein lysis buffer. A 10% SDS-PAGE gel was prepared, and equal amounts of protein samples were loaded onto the gel. The separated proteins were then transferred to a PVDF membrane (Millipore Corporation, Billerica, MA, USA)

Table 2 The primer sequence used in qRT–PCR

RNA	Primer
lincRNA-ASAO	(F) TCCGCCTCCTGGGTTCAAGTG
	(R) TGGCTGGGTGTGGTGGCTTAC
PTBP1	(F) AGCGCGTGAAGATCCTGTTC
	(R) CAGGGGTGAGTTGCCGTAG
DSPP	(F) TTTGGGCAGTAGCATGGGC
	(R) CCATCTTGGGTATTCTTTCCT
DMP1	(F) CTCCGAGTTGGACGATGAGG
	(R) TCATGCCTGCACTGTTTCATTC
ALPL exon 2 retained	(F) TCGATTGCATCTCTGGGCTC
	(R) GGTGCCAATGGCCAGTACTAA
ALPL exon 2 skipped	(F) CTGCGCAGAGAAAGAGAAAGAC
	(R) CACGTTGGTGTGAGCTTCTG

with a pore size of 0.22 µm. Non-specific binding sites on the membrane were blocked with 5% milk at room temperature for 1 h. The membrane was then incubated overnight at 4 °C with the following antibodies: glyceraldehyde-3-phosphate dehydrogenase (GAPDH) (Proteintech, 10,494–1-AP), dentin sialophosphoprotein (DSPP) (Bioword, BS71212), and dentin matrix protein 1 (DMP-1) (Affinity, DF8825, RRID: AB_2842022). The membrane was then incubated with appropriate secondary antibodies at room temperature for 1 h, before exposing using Immobilon Western Chemiluminescent HRP Substrate (Millipore Corporation, Billerica, MA, USA). The protein bands were quantitatively analyzed using ImageJ software or other suitable image analysis tools.

ALP staining

On the seventh day of hDPSC culture, alkaline phosphatase (ALP) activity staining was performed using the NBT/BCIP staining kit (Beyotime Biotech, Shanghai, China). Cells were washed three times with phosphate buffered saline (PBS) and fixed with 4% paraformaldehyde for 15 min. After washing, hDPSCs were stained using the NBT/BCIP staining kit (Beyotime Biotech, Shanghai, China). The results for each group were photographed under an inverted microscope.

Alizarin Red S (ARS) staining

On the seventh day of hDPSC culture, calcium nodule staining was performed using ARS staining solution. The cells were washed three times with PBS and fixed with 4% paraformaldehyde for 15 min. After washing, the cells were stained with ARS staining solution. The results for each group were photographed under an inverted microscope.

Rat dental pulp regeneration model construction

hDPSCs were transfected with lentivirus and divided into LV-NC group and LV-lincRNA-ASAO group. hDPSCs were prepared to 1.0×10^5 cells/ml in PBS. The cells were divided into PBS group, hDPSCs group, LV-NC group and LV-lincRNA-ASAO group. Each group contained five rats. Male SD rats aged 5–6 weeks weighing 150–180 g. All SD rats were raised in an SPF-level animal breeding center. Due to the small size of the experiment, a lottery was used for allocation. Each rat had an equal chance of being assigned to either group. The animal protocol was prepared before the study, and this protocol was registered in the hospital animal ethic committee (IACUC-LAC-20220712–004).

2.5% of tribromoethyl alcohol anesthesia, the left side of the maxillary first molar exposed pulp. The pulp tissue was cleaned, rinsed with normal saline and placed into cells. Then, iRoot BP and glass ionomer were used for pulp capping. Rats that died during the procedure were excluded, and the number of rats in each group was increased to five by the inclusion of new rats. Four weeks later, the rats were anesthetized with an overdose of tribromoethyl alcohol and sacrificed by neck amputation. The tissue samples from the left maxilla are used for subsequent staining. The procedures of animal experiments were compliant with the ARRIVE guidelines.

Masson staining

Place the paraffin sections in xylene to remove the wax. Gradually hydrate the sections through an ethanol gradient. Stain according to the instructions in the Mason's reagent kit. Rinse with distilled water to remove excess color. Dehydrate the sections through an ethanol gradient. Finally, immerse the sections in xylene for clearing. Cover the sections with a mounting medium and prepare for observation.

IHC staining

Paraffin sections were deparaffinized in xylene solution, then hydrated in a progressively decreasing concentration of alcohol solution, and finally rinsed with distilled water. Antigen repair was performed using sodium citrate buffer. The sections were treated using a milk blocking solution. The sections were incubated with the primary DSPP antibody (bs-10316R, Bioss) for 24 h at 4°C. Sections were treated with 3% hydrogen peroxide for 30 min. Unbound primary antibodies were removed by washing sections with TBS. The sections were incubated with a secondary antibody (PV-1022, Bioss). Unbound secondary antibodies were removed by washing sections with PBS. The addition of the chromogenic substrate DAB produced a color reaction. The nuclei were stained using hematoxylin. Dehydration was performed with a

concentration gradient of ethanol, followed by clearing with xylene, and finally the plates were sealed with neutral resin. The staining results were observed under a microscope, and image analysis and data recording were performed.

HE staining

Paraffin-embedded sections were deparaffinized with xylene and then hydrated through a gradient concentration of ethanol. This was followed by hematoxylin staining followed by eosin staining. After staining, sections were cleared, sealed, and then examined under a microscope.

RNA sequencing

After inducing stable hDPSC cell lines overexpressing lincRNA-ASAO, PTBP1, and their negative control for 14 days toward odontoblast-like cells, total transcriptome RNA was collected and sent to Ribobio Company (Guangzhou, China) for sequencing. Total RNA was extracted from hDPSCs using TRIzol reagent (15,596,018, Invitrogen). RNA quality was assessed using agarose gel electrophoresis, with samples having an RNA integrity number (RIN) > 7.0 selected for subsequent analysis. PolyA-seq technology was used to capture mRNA with 3' polyA tails in eukaryotes, detecting transcripts containing polyA tails. Sequencing was performed using Illumina NovaSeq 6000 with 150 bp paired-end reads. The raw sequencing data was quality assessed using FastQC and aligned to the reference genome with HISAT2. Differential expression analysis was performed using edgeR, with differentially expressed genes selected based on $|\log_2(\text{FoldChange})| > 1$ and $p < 0.05$. Functional annotation and pathway analysis were performed using clusterProfiler, with a significance threshold of $P < 0.05$, to identify enriched Gene Ontology (GO) terms and KEGG pathways for differentially expressed genes.

rMATs analysis

The RNA-Seq alignment results were processed using the rMATs software to perform differential splicing analysis. Specifically, rMATs calculates changes in various splicing events, including Skipped exon, Mutually exclusive exon, Alternative 5' splice site, Alternative 3' splice site, and Retained intron, using BAM files and annotation files. Differential splicing analysis employed a standard statistical model, with a threshold of $p < 0.05$ to filter out significantly different splicing events for further analysis of their biological significance.

Fluorescence in situ hybridization (FISH)

Cell climbing slice samples were collected and fixed on glass slides. The samples were preprocessed according

to the instructions (F12201, Genepharma) to enable the DNA to bind with the probes. We next prepared FITC-labeled lincRNA-ASAO probes complementary to the target lincRNA-ASAO sequence to be detected. The probes were incubated with the samples. After completing the hybridization of the probes and samples, the climbing slice was applied to subsequent IF experiments.

Immunofluorescence (IF)

IF experiments were conducted on cell climbing slices that underwent FISH. The slides were incubated with PTBP1 antibody (E4I3Q, Cell Signaling Technology) to bind to the intracellular PTBP1 protein, before washing away unbound antibodies and other impurities. CY3 fluorescent-labeled secondary antibody (ab6939, Abcam) was added to bind to the primary antibody, before washing away unbound secondary antibodies. The samples were observed using a fluorescence microscope, and fluorescence signals were detected at appropriate wavelengths.

RNA pull-down

An RNA pull-down KIT (Bes5102, China) was used for RPD detection according to the manufacturer’s instructions. The biotin-labeled lincRNA-ASAO probe and its antisense chain probe (BersinBio, China) were designed. Cell lysates from hDPSCs were collected and used in subsequent experiments after thorough lysis. The biotin-labeled probes were incubated with streptavidin-coated magnetic beads at room temperature for 25 min to form probe-bead complexes, which were then incubated with cell extracts at room temperature for 2 h to allow sufficient binding. The beads were washed five times in lysis buffer. Protein elution buffer was used to elute the proteins bound to the beads at 37 °C for 2 h. The separated protein samples on sodium dodecyl sulfate–polyacrylamide gel electrophoresis (SDS-PAGE) were selected for bands with differences and sent to allwegene (Beijing, China) for mass spectrometry analysis.

RNA immunoprecipitation (RIP) assay

According to the manufacturer’s instructions, the RNA immunoprecipitation (RIP) KIT (Bes5101, China) was used for RIP detection. Cell lysates prepared in buffer containing RNase inhibitor and protease inhibitor were precleared with PTBP1 antibody-coupled beads at 4 °C overnight. After washing with RIP wash buffer, the immunocomplexes bound to the beads were used for RNA isolation.

Photoactivatable-ribonucleoside-enhanced crosslinking and immunoprecipitation (PAR-CLIP)

By using the property of protein and RNA to undergo covalent cross-linking under 365 nm UV light, we

screened specific binding sites between protein PTBP1 and lincRNA-ASAO/ALPL pre-mRNA. According to the manufacturer’s protocol (BersinBio™ CLIP-qPCR Ki, Bes3014-1), the immunoprecipitation of the PTBP1-RNA binding complex was performed to obtain digested (with proteinase K, DNaseI, RNase T1) RNA, followed by RNA 3’ end adapter ligation and primer design for detecting the enrichment efficiency of RNA-binding protein sites.

Agarose gel electrophoresis

After obtaining RNA samples, reverse transcription was performed and specific primers were designed for PCR amplification (P112-01, Vazyme) to obtain DNA products. A 3% agarose gel was prepared and loaded into the electrophoresis chamber, before loading the sample mixtures into the gel wells. Gel electrophoresis was run at a constant voltage of 120 V for 30 min to allow DNA fragments to migrate according to their sizes. The gel was stained with a nucleic acid dye to visualize DNA bands. A UV gel imaging system was used to observe the DNA band patterns on the gel and estimate the sizes of the target DNA fragments based on the migration distance and standard sample sizes (Table 3).

Statistical analysis

Statistical analysis was performed using GraphPad Prism 9 to assess the differences between the groups. Statistical analysis of differences was conducted using a two-tailed Student’s *t*-test, with a *P*-value < 0.05 considered statistically significant.

Results

Characterization of lincRNA-ASAO

In our previous study [29], lncRNA microarray analysis was performed on hDPSCs after 14 days of odontoblastic induction to obtain a preliminary lncRNA expression profile. The screening criteria were set as follows: *P* < 0.05, fold change > 2, and abundance > 200. After screening, a novel lncRNA G018548 (named as an alternative splicing

Table 3 The primer sequence used in RT-PCR

RNA	Primer
ALPL-1	(F) CTATCTGGCTCCGTGCTC
	(R) CGCCAGTACTTGGGGTCTTT
ALPL-2	(F) GAGACCAAGCGCAAGAGACA
	(R) CCTTCACCCACACAGGTAG
ALPL-3	(F) CAGAAGCTCAACACCAACGTG
	(R) CCTTCACCCACACAGGTAG
COL11A1-1	(F) TGGAGTTCCAGGATTACCAGG
	(R) CCGTGACCTTTTCTCTCCAT
COL11A1-2	(F) CTCTGCTCAGGAAGCTCAGG
	(R) GTTAGACCCATTGGGCCAGG

associated odontoblastic differentiation lncRNA, lincRNA-ASAO) was obtained (Fig. 1A). LincRNA-ASAO, an intergenic lncRNA, is on human chromosome 12. RACE analysis revealed a transcript of lincRNA-ASAO, which was corrected from 744 to 1760 bp (Fig. 1B). The corrected sequence of lincRNA-ASAO was verified by gel electrophoresis of the RT-PCR products (Fig. 1C). The secondary structure of lincRNA-ASAO was visualized by RNAfold WEB (Fig. 1D). Three online tools, CPAT, NCBI, and CPC2, predicted that lincRNA-ASAO lacked protein coding potential (Fig. 1E). The validation results showed that the expression of lincRNA-ASAO increased with the extension of the induction time and reached a peak on day 14 (Fig. 1F). The expression of lincRNA-ASAO was also increased in human pulp tissues associated with deep caries compared to healthy tissues (Fig. 1G). FISH analysis was used to investigate the subcellular distribution of lincRNA-ASAO. In both hDPSCs and dental pulp tissue, lincRNA-ASAO was mainly expressed within the nucleus, especially in differentiated hDPSCs and dental pulp associated with deep caries (Fig. 1H, I).

Crucial roles of lincRNA-ASAO in odontogenesis

To evaluate the function of lincRNA-ASAO, lentiviral vectors were employed to overexpress or knock down lincRNA-ASAO in hDPSCs. Overexpression of lincRNA-ASAO resulted in increased ALP activity and enhanced calcium nodule deposition in hDPSCs, whereas knock-down of lincRNA-ASAO generated a decreased effect (Fig. 2A). Furthermore, the knockdown of lincRNA-ASAO led to decreased odontoblastic differentiation potential and reduced odontoblastic ability in hDPSCs. Overexpression of lincRNA-ASAO promoted the expression of odontoblastic-specific markers in hDPSCs (Fig. 2B–E). Therefore, our findings suggest that lincRNA-ASAO facilitates the odontoblastic differentiation of hDPSCs.

After differentiating into odontoblasts, hDPSCs in dental pulp tissue can secrete a matrix and mineralize to form reparative dentin, which protects the dental pulp from external stimuli. In this study, we established a rat model of *in situ* regeneration of dental pulp to investigate

whether overexpression of lincRNA-ASAO in hDPSCs can enhance the formation of reparative dentin. The flowchart is shown in Fig. 2F. HE and Masson's staining showed no obvious new dentin matrix or reparative dentin formation in the sham, control, or LV-NC groups. However, the overexpression of lincRNA-ASAO led to the obvious deposition of dentin matrix and reparative dentin on the pulp cavity wall. Moreover, immunohistochemistry revealed that the cells expressed more DSPP in the overexpression group (Fig. 2G). Therefore, our findings suggest that the expression of lincRNA-ASAO promotes the formation of reparative dentin *in vivo*.

LincRNA-ASAO interacts with PTBP1 protein

Interaction with specific proteins is an important mechanism for nuclear lncRNA to exert its function. Therefore, we conducted a preliminary exploration of the interacting proteins of lincRNA-ASAO. RNA pull-down experiments and the selection of differentially enriched bands for mass spectrometry analysis revealed several potential proteins that could be pulled down by lincRNA-ASAO. The enrichment results showed that these proteins are related to dentin regeneration (Fig. 3A and supplemental Fig. 1). To screen target proteins interacting with lincRNA-ASAO, the catRAPID website was used to predict the proteins interacting with lincRNA-ASAO. A comparison was made between the proteins with several detectable RNA-binding motifs in the predicted results and the proteins from the mass spectrometry results, resulting in the selection of the PTBP1 protein (Fig. 3B). Furthermore, from the prediction results, it was observed that most proteins contained only one RNA-binding motif, whereas PF00076 was the potential binding domain of PTBP1 with lincRNA-ASAO (Fig. 3C, D). Biotin-labeled RNA pull-down, followed by protein blotting analysis, was used to validate the interaction between lincRNA-ASAO and PTBP1 (Fig. 3E). The lincRNA-ASAO and PTBP1 may exert regulatory effects through two potential mechanisms: first, lincRNA-ASAO could impact the expression of PTBP1; second, lincRNA-ASAO may activate or inhibit the functional role of PTBP1. Experimental validation via western blotting demonstrated

(See figure on next page.)

Fig. 1 Identification and characterization of lincRNA-ASAO. **A** Flowchart illustrating the screening process for lincRNA-ASAO. Data were obtained from lncRNA microarray analysis performed on hDPSCs undergoing odontogenic differentiation for 14 days in a previous study. After setting the screening criteria as $P < 0.05$, fold change > 2 , and abundance > 200 , a unique lincRNA-ASAO was identified. **B** 5' RACE and 3' RACE were used to amplify the full length of lincRNA-ASAO. **C** Gel electrophoresis of RT-PCR products verified the corrected sequence of lincRNA-ASAO. **D** RNAfold was used to visualize the secondary structure of lincRNA-ASAO. **E** CPAT, NCBI, and CPC2 predict that lincRNA-ASAO lacks coding potential. **F** qRT-PCR was conducted to measure the expression levels of lincRNA-ASAO in hDPSCs undergoing odontogenic differentiation at 0, 3, 7, and 14 days. **G** qRT-PCR was conducted to measure the expression levels of lincRNA-ASAO in healthy and severely carious dental pulp. **H** FISH was performed to detect the intracellular localization of lincRNA-ASAO in hDPSCs before and after odontogenic differentiation. **I** FISH was performed to detect the intracellular localization of lincRNA-ASAO in healthy and severely carious dental pulp. * $P < 0.05$, ** $P < 0.01$, **** $P < 0.0001$

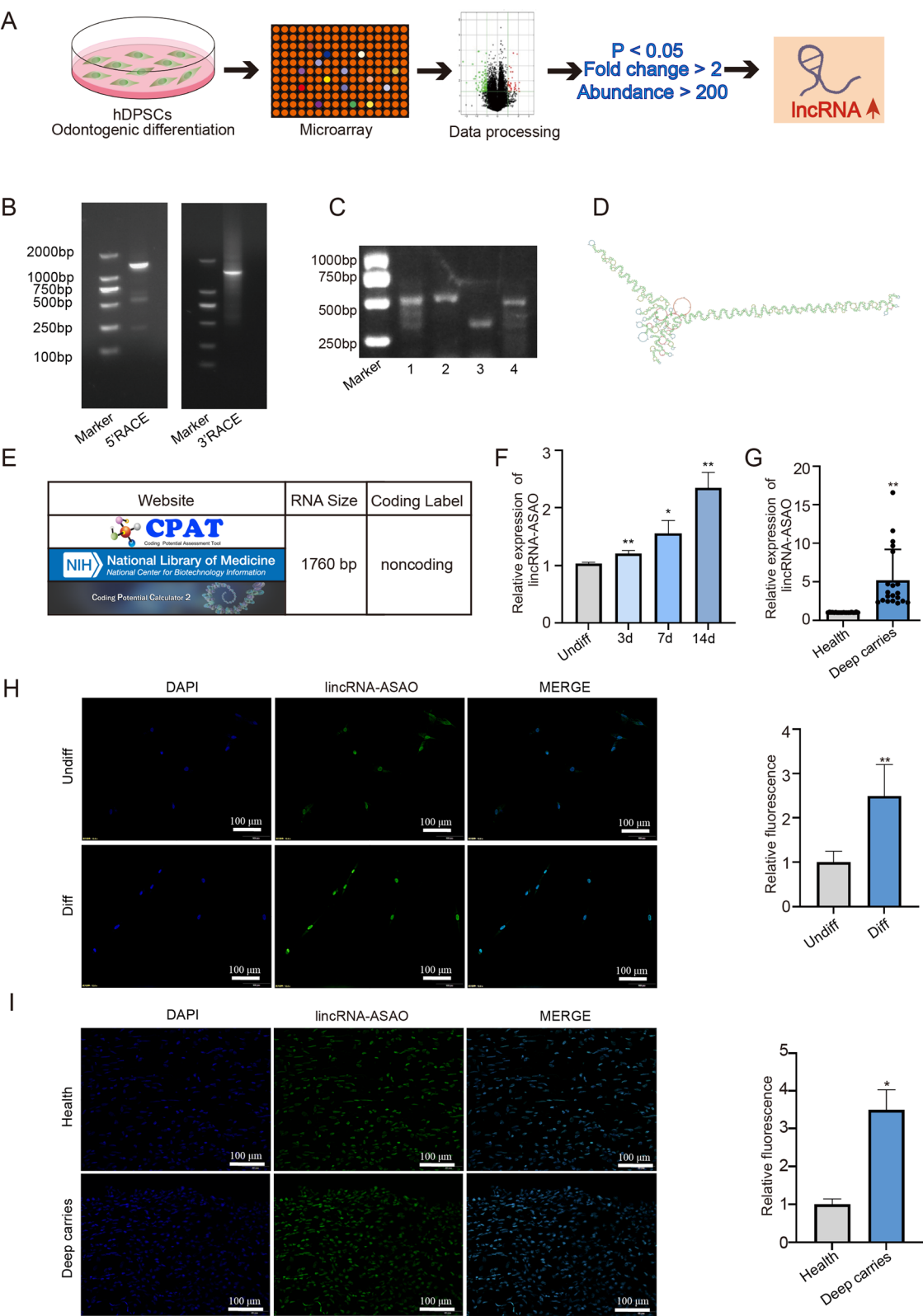


Fig. 1 (See legend on previous page.)

that lincRNA-ASAO did not influence the expression of PTBP1 (Fig. 3F). Therefore, the subsequent experiments was aim to investigate whether lincRNA-ASAO participates in the odontogenic differentiation of hDPSCs through its interaction with PTBP1.

We next determined the spatial localization information and specific binding sites of lincRNA-ASAO with PTBP1. FISH assay revealed that lincRNA-ASAO is located in the nucleus, whereas IF showed that PTBP1 is also localized in the nucleus. Moreover, lincRNA-ASAO and PTBP1 co-localized within the nucleus of hDPSCs before and after odontoblastic induction (Fig. 3G). In addition, RIP assays demonstrated that, compared to the control, the antibody targeting PTBP1 significantly enriched lincRNA-ASAO (Fig. 3H). In PAR-CLIP experiments, 10 primer pairs for lincRNA-ASAO were designed to verify the specific binding sites with PTBP1. The qRT-PCR results indicated successful amplification of the corresponding products for five primer pairs (289–309 bp, 947–969 bp, 1113–1133 bp, 1275–1294 bp, and 1374–1392 bp), suggesting a binding relationship between these sites and PTBP1 (Fig. 3I). In conclusion, PTBP1 was identified as an interacting partner of lincRNA-ASAO during the odontoblastic differentiation process of hDPSCs.

LincRNA-ASAO/PTBP1 promotes the odontoblastic differentiation of hDPSCs

Inhibition of PTBP1 using lentiviral vectors resulted in decreased ALP activity in hDPSCs and the formation of fewer calcium nodules. In addition, PTBP1 inhibition led to reduced levels of odontogenesis-related genes or proteins in hDPSCs, whereas PTBP1 overexpression enhanced the odontoblastic capabilities of hDPSCs (Fig. 4A–E). Therefore, it can be concluded that PTBP1 plays an important role in promoting the odontoblastic mechanisms in hDPSCs. Additionally, after co-transfection of sh-lincRNA-ASAO and LV-PTBP1, the co-transfected group did not exhibit a restoration of odontogenesis-related genes and proteins to normal induction levels (Fig. 4F, G). These findings suggest that

the function of LV-PTBP1 can be reversed by inhibiting lincRNA-ASAO.

ALPL pre-mRNA alternative splicing is regulated by lincRNA-ASAO/PTBP1

To screen for target genes associated with alternative splicing events regulated by lincRNA-ASAO-mediated PTBP1, RNA high-throughput sequencing was performed on hDPSCs that overexpressed lincRNA-ASAO and PTBP1 after odontoblastic induction. First, differentially expressed genes were identified in the lincRNA-ASAO overexpression group and PTBP1 overexpression group (Fig. 5A, B). Subsequently, rMATS analysis was conducted to identify alternative splicing events in the lincRNA-ASAO and PTBP1 groups, with exon skipping being the most abundant event (Fig. 5C). A total of 12 common alternative splicing events involving 10 mRNAs were identified. Next, 64 similar differentially expressed genes were screened between the lincRNA-ASAO and PTBP1 groups (Fig. 5D). GO functional analysis of these genes revealed three relevant terms associated with odontoblastic differentiation, including skeletal system morphogenesis, ossification, and positive regulation of ossification (Fig. 5E). Five genes (SOX11, OXT, SFRP2, ALPL, and COL11A1) were extracted from these terms. Through further screening, ALPL and COL11A1 were selected as target pre-mRNAs (Fig. 5F). By screening the common genes between the 10 mRNAs with similar splicing events and the 5 genes related to odontoblast differentiation, ALPL and COL11A1 are finally selected as potential target pre-mRNAs (Fig. 5F).

Further analysis revealed that ALPL had three potential exon-skipping events, whereas COL11A1 had two potential exon-skipping events. Primers were designed targeting both ends of the skipped exons, and RNA was amplified from lincRNA-ASAO-overexpressing and PTBP1-overexpressing cells. Gel electrophoresis imaging revealed that both ALPL and COL11A1 exhibited exon skipping. Compared to the control group, only the second exon of ALPL showed exon skipping (Fig. 5G, H and supplemental Fig. 2). Further quantitative analysis demonstrated a significant difference in exon skipping relative

(See figure on next page.)

Fig. 2 LincRNA-ASAO promoted the odontogenesis of hDPSCs. **A** ALP and ARS staining showed that lincRNA-ASAO knockdown decreased ALP activity and calcium nodule deposition in hDPSCs, while lincRNA-ASAO overexpression resulted in opposite outcomes. **B, C** Knockdown of lincRNA-ASAO reduced the expression of odontogenesis-related genes and proteins. Full-length blots are presented in Supplementary Fig. 3. **D, E** Overexpression of lincRNA-ASAO promoted the expression of odontogenesis-related genes and proteins. Full-length blots are presented in Supplementary Fig. 3. **F** The process of establishing an in situ regeneration model of dental pulp in rats, including pulp opening, root canal preparation, and implanted cells + iRoot BP + Glc in the maxillary first molar. The groups included the PBS group, PBS + hDPSCs group, PBS + LV-NC hDPSCs group, and PBS + LV-lincRNA-ASAO hDPSCs group. **G** HE and Masson's staining showed that compared to the control group, the hDPSC group overexpressing lincRNA-ASAO formed more dental pulp matrix or reparative dentin. Similarly, immunohistochemistry showed that overexpression of lincRNA-ASAO in the hDPSC group led to increased DSPP expression. * $P < 0.05$, ** $P < 0.01$, **** $P < 0.0001$

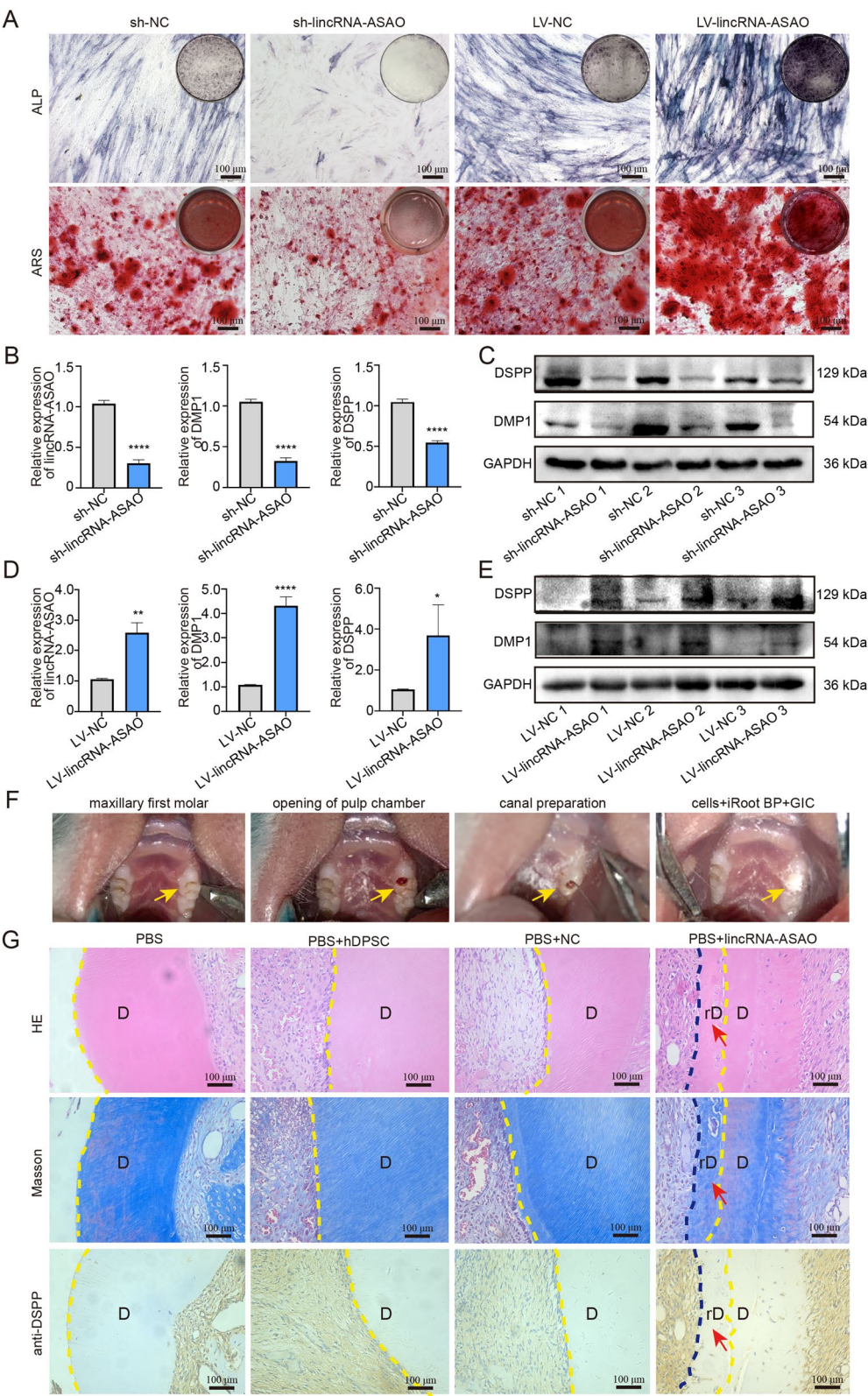


Fig. 2 (See legend on previous page.)

to exon retention in the second exon of ALPL between the lincRNA-ASAO and PTBP1 overexpression groups (Fig. 5I, J). Therefore, lincRNA-ASAO, in conjunction with PTBP1, regulates the exon skipping of ALPL pre-mRNA at its second exon.

Interaction sites between lincRNA-ASAO, PTBP1, and ALPL pre-mRNA

To explore the detailed mechanisms of lincRNA-ASAO, PTBP1, and ALPL pre-mRNA, the potential interaction sites between these three components were elucidated. Because the length of ALPL pre-mRNA is 69,752 bp, we conducted comprehensive and detailed binding site prediction between lincRNA-ASAO and ALPL pre-mRNA using RIssearch. The prediction results showed that there were highly probable sequences within the region of 1000–1700 bp that could bind to lincRNA-ASAO. This segment of sequence corresponds to the stem structure at the 3' end of the lincRNA-ASAO secondary structure. The majority of the binding sites on ALPL pre-mRNA were located in introns 1 and 2, with almost all of the first 20 binding sites falling within these two introns. Interestingly, these two introns are exactly adjacent to exon 2 of ALPL (Table 4). On the basis of the aforementioned predictions, we speculate that lincRNA-ASAO uses its stable stem structure to recognize and pair with introns 1 and 2 on ALPL pre-mRNA, providing targeted guidance for the regulatory function of PTBP1.

When hnRNPs interact with exonic splicing silencer (ESS) on pre-mRNA, it can enhance the recognition and splicing efficiency of the splicing complex, leading to exon skipping (Fig. 6A). We hypothesize that PTBP1 is capable of recognizing and interacting with the ESS sequence on exon 2 of ALPL pre-mRNA, thereby influencing exon skipping events. First, based on the prediction results from catRAPID, we found that three domains (PF00076, PF11835, and PF13893) on PTBP1 might bind to exon 2 of ALPL pre-mRNA (Fig. 6B–E). In addition, according to the prediction results from RBPsuite, the latter half of the sequence of exon 2 of ALPL pre-mRNA

is likely to interact with PTBP1 (Fig. 6F). Further predictions from SpliceAid indicated the presence of numerous ESS sites on exon 2 of ALPL pre-mRNA, with these sites predominantly rich in CU content (Fig. 6G). Subsequently, we conducted PAR-CLIP experiments to validate the existence of ESS sequences on exon 2 of ALPL pre-mRNA that interact with PTBP1. The qRT–PCR results demonstrated that PTBP1 can interact with the ESS sequence on exon 2 (Fig. 6H). Therefore, we propose that lincRNA-ASAO might recognize and pair with ALPL pre-mRNA, guiding the interaction between PTBP1 and the ESS sequence on exon 2 of ALPL pre-mRNA. This interaction might enhance PTBP1's recognition and splicing efficiency of exon 2 by PTBP1, leading to exon skipping (Fig. 6I).

Discussion

Selective splicing is a crucial cellular process that generates multiple splice variants, thereby regulating gene expression and functional diversity. These isoforms can influence cellular activities and determine the fate of cells to some extent [30–33]. However, the role of alternative splicing in reparative dentinogenesis has received little attention in dental pulp repair processes. In this study, we identified a novel lincRNA-ASAO and discovered a new regulatory mechanism mediated by this lncRNA in modulating alternative splicing of target genes, marking the first report of lncRNA affecting dental pulp repair through the regulation of target gene alternative splicing. Our results indicate that lincRNA-ASAO interacts with PTBP1, regulating alternative splicing of downstream odontogenesis-related genes.

Nucleic acid drugs are a new generation of gene editing technologies that have become a research hotspot in the field of new drug development due to their efficiency and rapid action. Several nucleic acid drugs have entered clinical trials, with some already approved for treatment in different fields [34]. Given the critical role of lincRNA-ASAO in dental pulp repair, targeting lincRNA-ASAO could become a potential therapeutic strategy to promote

(See figure on next page.)

Fig. 3 Screening and identification of target proteins for lincRNA-ASAO. **A** Pull-down assay was performed using probes targeting lincRNA-ASAO and its antisense chain to capture potential binding proteins, followed by SDS-PAGE and silver staining. Bands showing differential expression were selected for mass spectrometry identification. **B–D** The catRAPID prediction identified proteins that may interact with lincRNA-ASAO, among which proteins containing the most detected RNA-binding motifs were selected. Among these, PTBP1 was identified through union screening of proteins detected in the pull-down results. **E** Western blotting identified the protein in the RNA pulldown sample, indicating that the lincRNA-ASAO probe can bind to the protein PTBP1. Full-length blots are presented in Supplementary Fig. 3. **F** Western blotting demonstrated that lincRNA-ASAO does not influence the expression of PTBP1. Full-length blots are presented in Supplementary Fig. 3. **G** The combined FISH and IF experiments indicated that lincRNA-ASAO and PTBP1 co-localized within the nucleus of hDPSCs both before and after odontoblastic induction. **H** RIP assays demonstrated that the antibody targeting PTBP1 significantly enriched lincRNA-ASAO compared to the control. **I** PAR-CLIP was used to screen for RNA fragments specifically bound to PTBP1. qRT–PCR was employed to identify the binding sites of lincRNA-ASAO and PTBP1 in the PAR-CLIP result samples. ** $P < 0.01$, *** $P < 0.001$

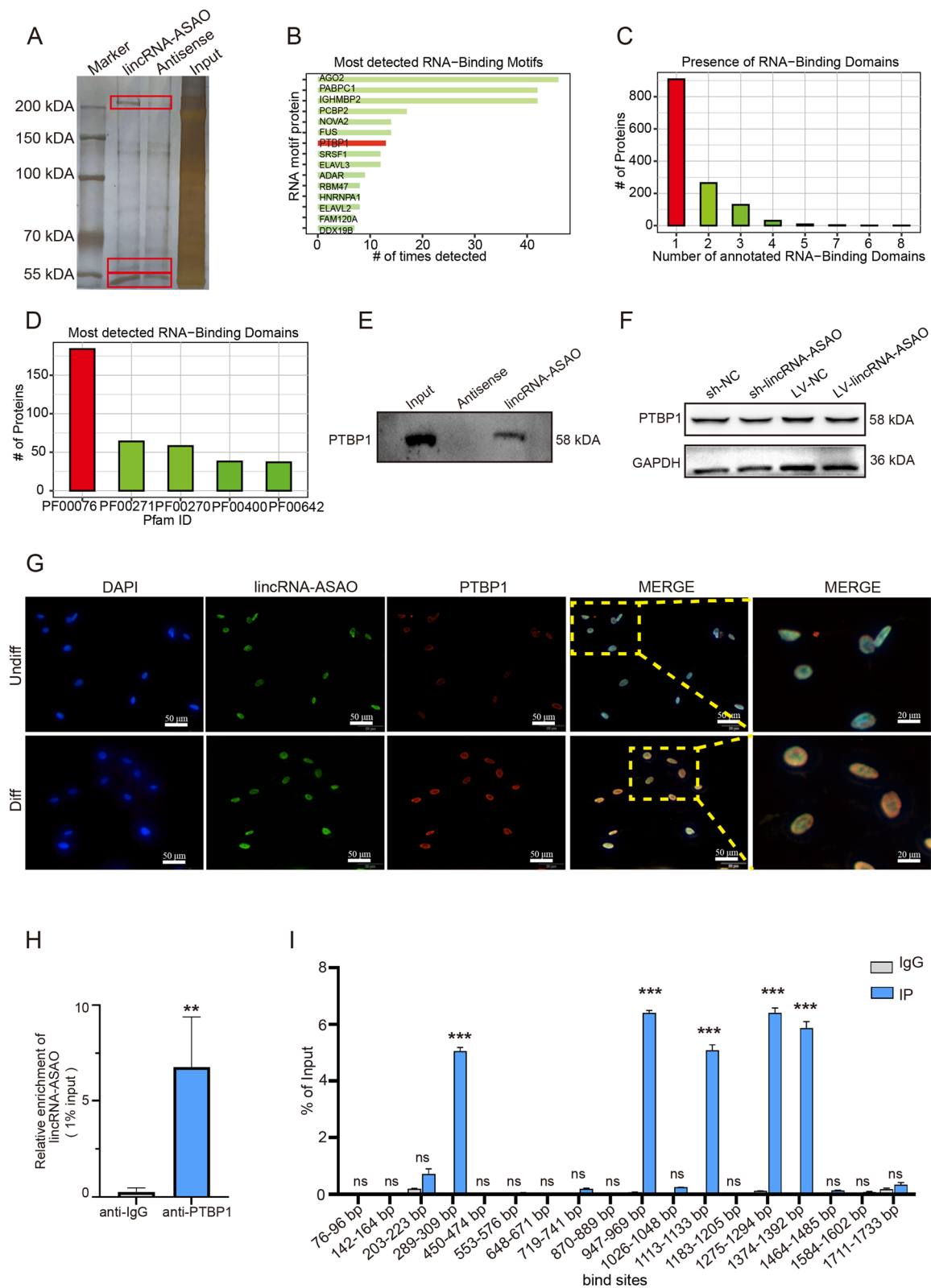


Fig. 3 (See legend on previous page.)

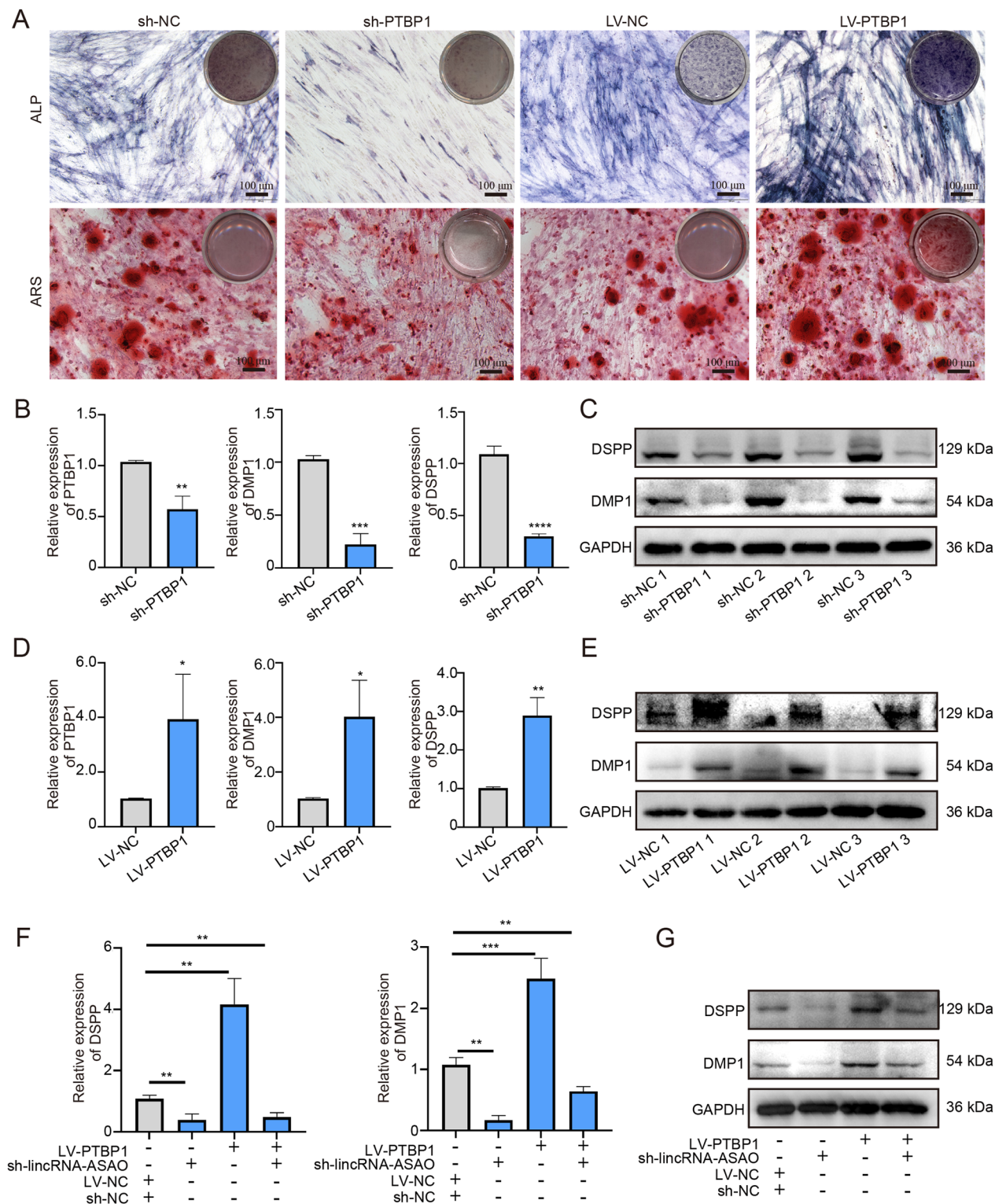


Fig. 4 PTBP1 is involved in lncRNA-mediated odontoblastic differentiation of hDPSCs. **A** ALP and ARS staining revealed that PTBP1 knockdown led to reduced ALP activity and calcium nodule deposition in hDPSCs, while PTBP1 overexpression yielded opposite outcomes. **B, C** Knockdown of PTBP1 resulted in decreased expression of odontogenesis-related genes or proteins in hDPSCs. Full-length blots are presented in Supplementary Fig. 3. **D, E** Overexpression of PTBP1 promoted higher levels of odontogenesis-related genes or proteins in hDPSCs. Full-length blots are presented in Supplementary Fig. 3. **F, G** Inhibiting the expression of lincRNA-ASAO can reverse the promotion of odontogenic differentiation function by PTBP1. Full-length blots are presented in Supplementary Fig. 3. * $P < 0.05$, ** $P < 0.01$, *** $P < 0.001$, **** $P < 0.0001$

pulp repair. According to the current application methods of lncRNA as nucleic acid drugs, targeting lincRNA-ASAO can be applied through various approaches. Artificially synthesized lincRNA-ASAO or its analogs can be used to promote pulp repair by targeting PTBP1 [35]. In addition, RNA interference technology can be employed to specifically inhibit the function of lincRNA-ASAO using small interfering RNA, altering the variable splicing events of ALPL, and further influencing the dentin formation process [36]. Additionally, combining gene editing tools like CRISPR/Cas9 for precise editing of lincRNA-ASAO can regulate its role in pulp repair [37]. At the same time, delivery systems such as nanoparticles, liposomes, or viral vectors can be used to ensure that lincRNA-ASAO or its regulatory molecules efficiently enter pulp cells, enhancing their repair effects [38]. Through these approaches, targeting lincRNA-ASAO holds promise as a new therapeutic strategy for pulp repair. However, like other nucleic acids, lincRNA-ASAO faces several challenges in application, including low stability, short half-life, high immunogenicity, and endosomal escape [34].

Studying lncRNAs presents unique challenges, particularly due to the limitations of short-read RNA sequencing in accurately determining lncRNA transcripts, especially in cases with complex subtypes [39, 40]. In this study, we employed RACE and cloning techniques to identify the transcript of lincRNA-ASAO and detected only one subtype. The lincRNA-ASAO sequence was determined using long-read sequencing, which revealed partial similarities to known sequences, but with updated sequences at both ends. Our findings demonstrate that lincRNA-ASAO possesses a single subtype during hDPSC odontoblastic differentiation. In addition, we did not examine lincRNA-ASAO in other species and therefore cannot determine its conservation. In recent years, many lncRNAs have been found to play important roles in the odontogenic differentiation of DPSCs. Most of these lncRNAs regulate odontogenic differentiation of DPSCs through the ceRNA mechanism [41–47], but research on other regulatory mechanisms is still limited. In our study, lincRNA-ASAO regulates the alternative splicing

of odontogenic-related genes by binding to PTBP1. This finding reveals a new mechanism in the odontogenic differentiation of DPSCs. Since PTBP1 is a splicing factor commonly found in various cells [48], and ALPL is a key marker in osteogenic differentiation [49], we speculate that lincRNA-ASAO may be a key molecule in regulating the osteogenic differentiation of stem cells. However, the specific transcript and regulatory mechanism of lincRNA-ASAO in other cells still need further experimental verification.

Although most lncRNAs function primarily at the RNA level, some have been discovered to possess the capacity to translate into peptides. In this study, we initially predicted that lincRNA-ASAO lacks coding ability and therefore likely functions primarily at the RNA level. Our experiments confirmed that lincRNA-ASAO acts primarily as a mechanistic molecule in hDPSCs. However, certain studies have suggested that specific lncRNAs undergo translation under particular conditions, resulting in functional peptide segments [50, 51]. Consequently, we must consider this aspect in our research and further explore the dual functional mechanism of lncRNAs to gain a more comprehensive understanding of their roles in various physiological and pathological processes.

Numerous studies have demonstrated that lncRNAs play a regulatory role in alternative splicing by forming RNA-RNA duplexes with pre-mRNA [52–54]. This process typically involves lncRNAs targeting specific splicing factors to cis-regulatory nucleotide sequences [52, 55]. For example, lncRNA SAF binds to the junction of exon 5–6 and exon 6–7 of Fas pre-mRNA, associating with SPF45 and promoting exon 6 skipping [54]. In addition, lncRNA zinc finger E-box binding homeobox 2 antisense RNA 1 (ZEB2-AS1) forms an RNA-RNA duplex with ZEB2 pre-mRNA, resulting in retention of the ZEB 5′-UTR intron [53]. The formation of an RNA-RNA duplex by lncRNA PLANE and NCOR2 pre-mRNA facilitates hnRNP binding to intron 45 of the precursor mRNA, thereby inhibiting alternative splicing events for NCOR2-202 [56]. In this study, we investigated the potential and specific sites of lincRNA-ASAO forming

(See figure on next page.)

Fig. 5 lincRNA-ASAO/PTBP1 regulates alternative splicing of ALPL. **A** High-throughput RNA sequencing was conducted on the NC and lincRNA-ASAO groups. Heatmaps were generated to illustrate the differential mRNA expression in the sequencing results. **B** High-throughput RNA sequencing was conducted in the overexpression NC and PTBP1 groups. Heatmaps were generated to illustrate the differential mRNA expression in the sequencing results. **C** rMATS analysis identified alternative splicing events in the overexpressed lincRNA-ASAO and PTBP1 groups, with exon skipping being the most abundant event. **D** A heatmap was generated to display the 64 common differentially expressed mRNAs between the overexpression lincRNA-ASAO and PTBP1 groups. **E** GO analysis of 64 common differentially expressed mRNAs. **F** Flowchart of the screening process for ALPL and COL11A1. **G, H** We designed primers spanning exons for PCR amplification to obtain products, which were then subjected to agarose gel electrophoresis. Exon skipping was determined based on the size of the amplified products. **I, J** Specific primers were designed based on the exon skipping status. qRT-PCR quantified the significant difference in exon 2 skipping of ALPL premRNA. * $P < 0.05$

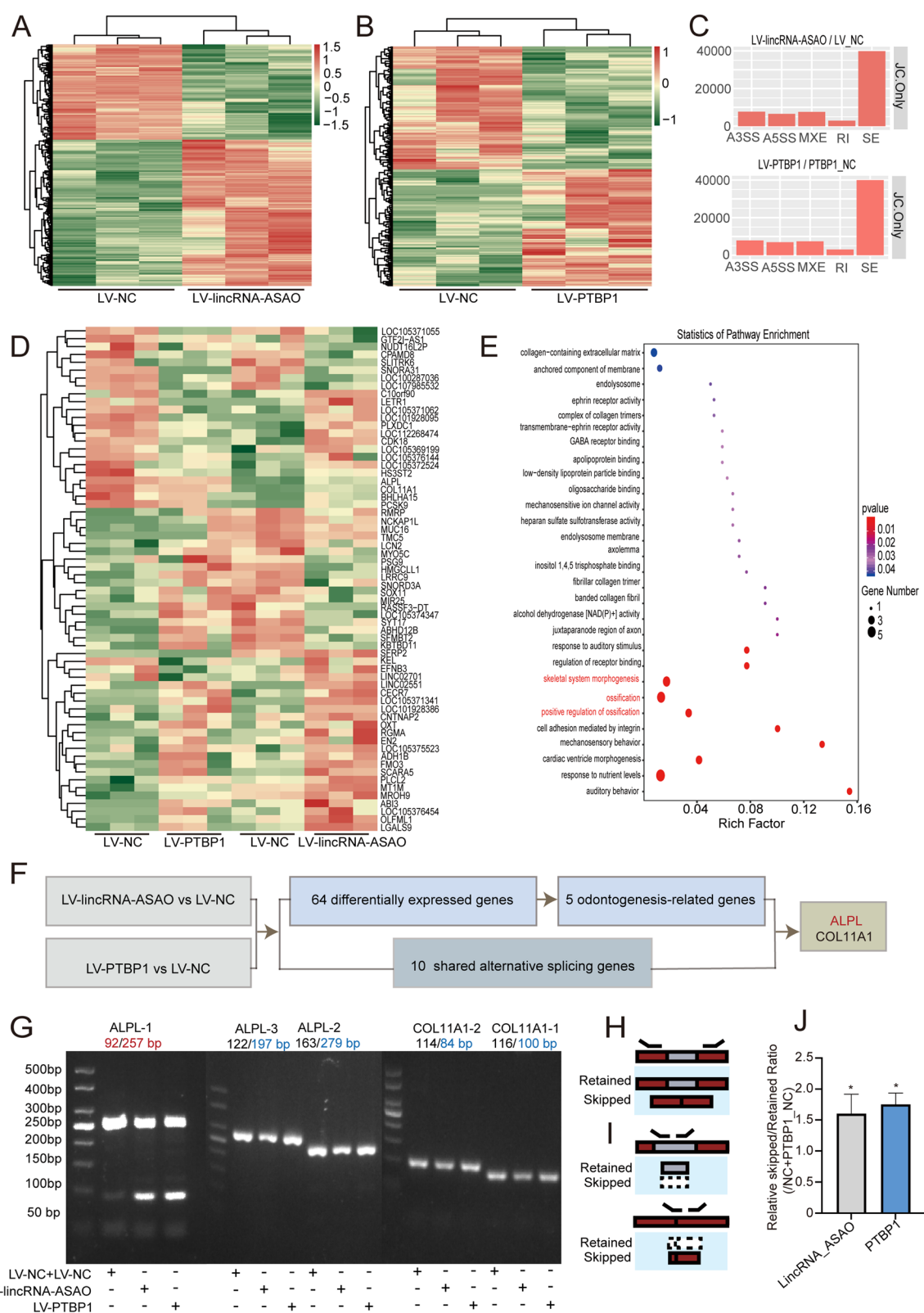


Fig. 5 (See legend on previous page.)

Table 4 Rlsearch predicts the binding sites of lincRNA-ASAO with ALPL pre-mRNA

RNA	Star	End	RNA	Star	End	Intron
lincRNA-ASAO	1528	1726	ALPL pre-mRNA	17635	17830	1
	1525	1743		40058	40264	1
	1527	1724		46374	46572	2
	1528	1720		42331	42525	1
	1525	1720		11789	11986	1
	1531	1720		27500	27693	1
	1528	1722		46023	46216	2
	1527	1725		45095	45291	1
	1528	1710		22810	22989	1
	1471	1645		46454	46628	2

duplexes with ALPL pre-mRNA. Intriguingly, the stable stem-loop region of lincRNA-ASAO can interact with the first and second introns of ALPL pre-mRNA. Our prediction results suggest that lincRNA-ASAO targets PTBP1 to the ESS sequence adjacent to the second exon of ALPL pre-mRNA. However, further research is required to elucidate the formation and specific mechanism of this duplex.

In general, hnRNPs regulate the alternative splicing of various pre-mRNAs in a sequence-dependent manner, with these regulatory sequences located within exons or introns [57, 58]. When exon skipping occurs, hnRNP may bind to the ESS and convey the message to the spliceosome, indicating that the site should not be spliced, ultimately resulting in exon skipping. Certain ESS sequences have been identified for specific hnRNPs [59–61]. For example, the binding of hnRNP A1 to ESS results in exon 17 skipping in SMN [62]. Furthermore, hnRNP H1/F binds to ESS and modulates the alternative splicing of TCF3 [63]. Our study revealed that PTBP1 binds to the ESS sequence of exon 2 in ALPL pre-mRNA and is involved in lincRNA-ASAO-mediated exon skipping. Notably, this ESS sequence is rich in CU, which further confirms the high affinity of PTBP1 for RNA sequences rich in CU and aligns with previous research findings.

Our study still has some mechanisms that require further experimental validation. Based on the existing

research results, it is reasonable to speculate that the interaction between lincRNA-ASAO and PTBP1 affects ALPL exon skipping and the differentiation process of hDPSCs. The experimental results also suggest the specific binding sites of lincRNA-ASAO and PTBP1. However, further experiments are needed to mutate these sites in order to clarify the key binding sites between lincRNA-ASAO and PTBP1 during the odontogenic differentiation process of hDPSCs, as well as to determine the direct role of the lincRNA-ASAO-PTBP1 interaction in driving ALPL exon skipping and promoting hDPSCs differentiation.

Conclusions

This study provides preliminary insights into the regulation of alternative splicing in target genes by lncRNA and its impact on the odontoblastic differentiation of hDPSCs. Our findings demonstrate that lincRNA-ASAO is expressed as a single isoform during the odontoblastic differentiation of hDPSCs and enhances their capacity for odontoblastic differentiation. The interaction between lincRNA-ASAO and PTBP1 might play a regulatory role in the alternative splicing of ALPL pre-mRNA, which is associated with odontogenesis. Therefore, the newly discovered lincRNA-ASAO can represent a critical target for dental pulp repair and regeneration.

(See figure on next page.)

Fig. 6 Interaction sites between lincRNA-ASAO, PTBP1, and ALPL pre-mRNA. **A** Schematic illustrating how hnRNP proteins can regulate exon skipping by binding to ESS sequences in premRNA. **B–E** catRAPID predicted that three domains (PF00076, PF11835, and PF13893) within PTBP1 bind to the second exon of ALPL premRNA. **F** RBPsuite predicts the potential binding sequences of ALPL premRNA exon 2 to PTBP1. **G** SpliceAid predicts potential ESS sequences in ALPL premRNA exon 2. **H** PAR-CLIP experiments obtained RNA fragments that bind to PTBP1. qRT-PCR results demonstrated that PTBP1 can interact with the ESS sequence in exon 2. **I** LincRNA-ASAO may recognize and pair with ALPL pre-mRNA, guiding the interaction between PTBP1 and the ESS sequence on exon 2 of ALPL pre-mRNA. This interaction may enhance PTBP1’s recognition and splicing efficiency of exon 2 by PTBP1, leading to exon skipping. ****P* < 0.001

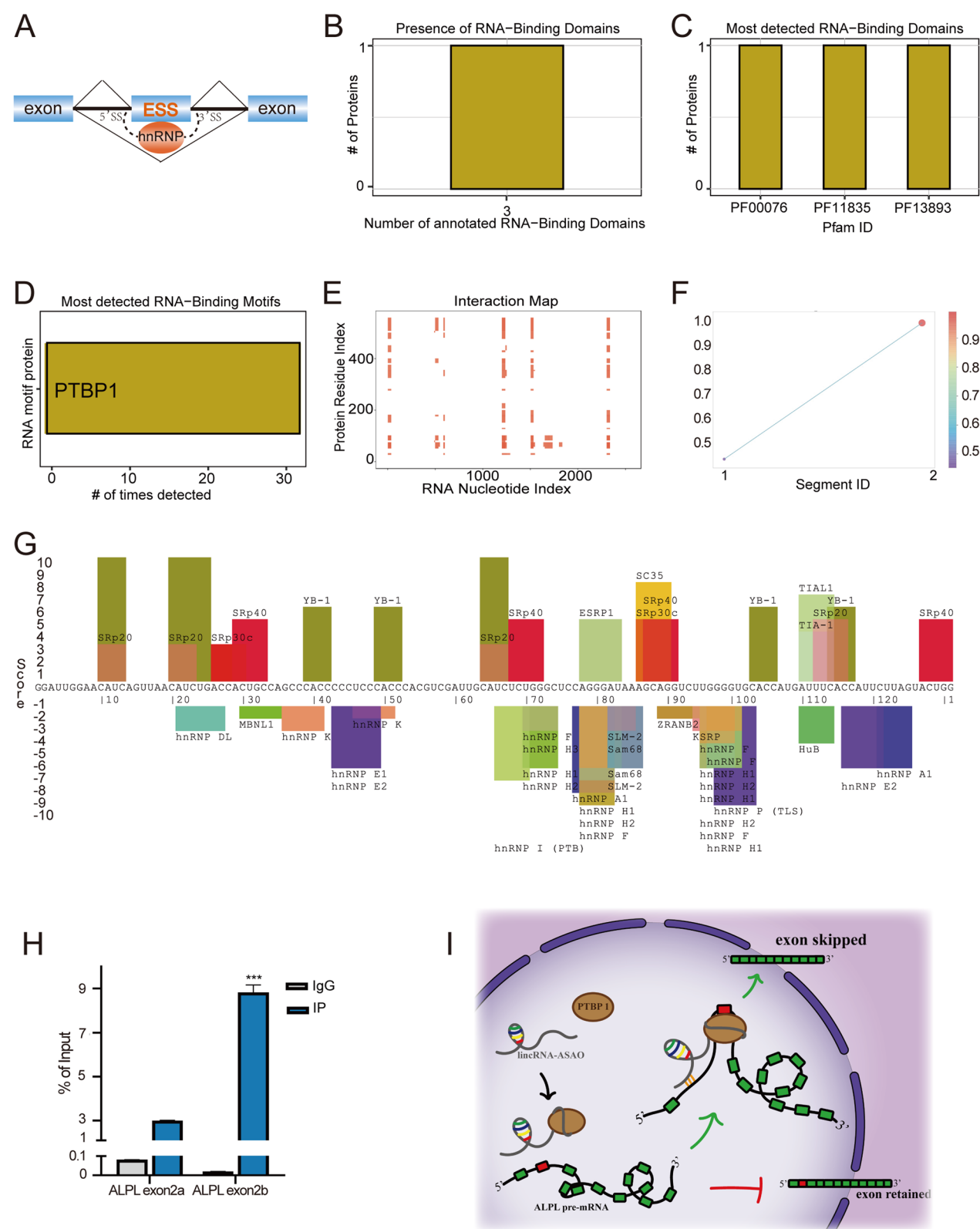


Fig. 6 (See legend on previous page.)

Abbreviations

LincRNA-ASAO	Intergenic lncRNA Alternative Splicing-Associated Odontoblastic differentiation
hDPSCs	Human Dental Pulp Stem Cells
hnRNP	Heterogeneous nuclear ribonucleoprotein
PTBP1	Polypyrimidine Tract Binding Protein 1
DSPP	Dentin Sialophosphoprotein
DMP1	Dentin Matrix Acidic Phosphoprotein 1
ALPL	Alkaline Phosphatase
PAR-CLIP	Photoactivatable-Ribonucleoside-Enhanced Crosslinking and Immunoprecipitation
ESS	Exonic splicing silencer
FISH	Fluorescence in situ hybridization
IF	Immunofluorescence

Supplementary Information

The online version contains supplementary material available at <https://doi.org/10.1186/s13287-025-04274-w>.

Supplementary file1

Acknowledgements

We thank LetPub (www.letpub.com) for its linguistic assistance during the preparation of this manuscript.

Author contributions

Buling Wu, Zhao Chen, Wei Qiu, Fuchun Fang and Xiaolan Guo conceived and designed the study. Xiaolan Guo, Sitong Liu, Longrui Dang and Cheng Zeng conducted the experiments and administered the data. Xiaolan Guo, Sitong Liu, Longrui Dang, Lu Chen, Zehao Chen, Yumeng Yang and Jiahao Lin performed the experiments. Buling Wu, Zhao Chen, Wei Qiu, Fuchun Fang and Xiaolan Guo interpreted the data and wrote the manuscript. All the authors have read and approved the final manuscript.

Funding

This work was supported by the National Natural Science Foundation of China (82270982, 82100996, 82101024, 82170942), the Natural Science Foundation of Guangdong Province (2024A1515010840), the Guangzhou Science and Technology Plan Project (2024B03J0667, 2024A04J5188, 2024A04J5105), Funding by Science and Technology Projects in Guangzhou (2024B03J0667), President Foundation of Shenzhen Stomatology Hospital (Pingshan) of Southern Medical University (714004) and the Fundamental research project of Shenzhen Science and Technology Innovation Committee (JCYJ20210324121007020).

Availability of data and materials

The authors confirm that the data supporting the findings of this study are available within the article and its supplementary materials. The raw sequence data reported in this paper have been deposited in the NCBI Sequence Read Archive (PRJNA1208419).

Declarations

Ethics approval and consent to participate

The project titled "The study on the mechanism of lncRNA G018548 binding to PTBP1 to regulate odontoblastic differentiation of human dental pulp stem cells" has been reviewed and approved by two ethical committees at Nanfang Hospital, Southern Medical University. The Animals Ethics Committee granted approval under the number IACUC-LAC-202207 12-004 in July 2022. Additionally, the Medical Ethics Committee approved the project under approval number NFEC-202302-K5-01 in February 2023. The patients provided written informed consent for participation in the study and the use of samples.

Consent for publication

Not applicable.

Competing interests

The authors declare that they have no competing interests.

Use of AI tools declaration

The authors declare that they have not use AI-generated work in this manuscript.

Author details

¹Department of Stomatology, Nanfang Hospital, Southern Medical University, Guangzhou, China. ²Shenzhen Stomatology Hospital (Pingshan), Southern Medical University, Shenzhen, China. ³Shenzhen Clinical College of Stomatology, School of Stomatology, Southern Medical University, Guangzhou, China.

Received: 12 January 2025 Accepted: 11 March 2025

Published online: 26 March 2025

References

- Keren H, Lev-Maor G, Ast G. Alternative splicing and evolution: diversification, exon definition and function. *Nat Rev Genet*. 2010;11:345–55.
- Pozo F, Martinez-Gomez L, Walsh TA, Rodriguez JM, Di Domenico T, Abascal F, et al. Assessing the functional relevance of splice isoforms. *NAR Genom Bioinform*. 2021;3: b44.
- Rodriguez JM, Pozo F, di Domenico T, Vazquez J, Tress ML. An analysis of tissue-specific alternative splicing at the protein level. *Plos Comput Biol*. 2020;16: e1008287.
- Pan Q, Shai O, Lee LJ, Frey BJ, Blencowe BJ. Deep surveying of alternative splicing complexity in the human transcriptome by high-throughput sequencing. *Nat Genet*. 2008;40:1413–5.
- Wang ET, Sandberg R, Luo S, Khrebukova I, Zhang L, Mayr C, et al. Alternative isoform regulation in human tissue transcriptomes. *Nature*. 2008;456:470–6.
- Shepard PJ, Hertel KJ. The SR protein family. *Genome Biol*. 2009;10:242.
- Biamonti G, Caceres JF. Cellular stress and RNA splicing. *Trends Biochem Sci*. 2009;34:146–53.
- Li D, Yu W, Lai M. Towards understandings of serine/arginine-rich splicing factors. *Acta Pharm Sin B*. 2023;13:3181–207.
- Singh R, Valcárcel J. Building specificity with nonspecific RNA-binding proteins. *Nat Struct Mol Biol*. 2005;12:645–53.
- Rogalska ME, Vivori C, Valcárcel J. Regulation of pre-mRNA splicing: roles in physiology and disease, and therapeutic prospects. *Nat Rev Genet*. 2023;24:251–69.
- Fiszbein A, Kornbliht AR. Alternative splicing switches: Important players in cell differentiation. *BioEssays*. 2017;39(6):1600157.
- Fu RH, Liu SP, Ou CW, Yu HH, Li KW, Tsai CH, et al. Alternative splicing modulates stem cell differentiation. *Cell Transplant*. 2009;18:1029–38.
- Yabas M, Elliott H, Hoyne GF. The role of alternative splicing in the control of immune homeostasis and cellular differentiation. *Int J Mol Sci*. 2015. <https://doi.org/10.3390/ijms17010003>.
- Olivieri JE, Dehghannasiri R, Wang PL, Jang S, de Morree A, Tan SY, et al. RNA splicing programs define tissue compartments and cell types at single-cell resolution. *Elife*. 2021. <https://doi.org/10.7554/eLife.70692>.
- Shi Y. Mechanistic insights into precursor messenger RNA splicing by the spliceosome. *Nat Rev Mol Cell Biol*. 2017;18:655–70.
- Pritsker M, Doniger TT, Kramer LC, Westcot SE, Lemischka IR. Diversification of stem cell molecular repertoire by alternative splicing. *Proc Natl Acad Sci U S A*. 2005;102:14290–5.
- Salomonis N, Schlieve CR, Pereira L, Wahlquist C, Colas A, Zamboni AC, et al. Alternative splicing regulates mouse embryonic stem cell pluripotency and differentiation. *Proc Natl Acad Sci U S A*. 2010;107:10514–9.
- Gronthos S, Mankani M, Brahimi J, Robey PG, Shi S. Postnatal human dental pulp stem cells (DPSCs) in vitro and in vivo. *Proc Natl Acad Sci U S A*. 2000;97:13625–30.
- Qian Y, Gong J, Lu K, Hong Y, Zhu Z, Zhang J, et al. DLP printed hDPSC-loaded GelMA microsphere regenerates dental pulp and repairs spinal cord. *Biomaterials*. 2023;299: 122137.
- Liang X, Xie L, Zhang Q, Wang G, Zhang S, Jiang M, et al. Gelatin methacryloyl-alginate core-shell microcapsules as efficient delivery platforms for prevascularized microtissues in endodontic regeneration. *Acta Biomater*. 2022;144:242–57.
- Shen J, She W, Zhang F, Guo J, Jia R. YBX1 promotes the inclusion of RUNX2 alternative exon 5 in dental pulp stem cells. *Int J Stem Cells*. 2022;15:301–10.

22. Zhang Y, Huang J, Yan L, Jia R, Guo J. HnRNP A1 suppresses the odontogenic differentiation and the inclusion of RUNX2 Exon 5 of dental mesenchymal cells. *Front Biosci (Landmark Ed)*. 2023;28:139.
23. Feng Z, Li Q, Meng R, Yi B, Xu Q. METTL3 regulates alternative splicing of MyD88 upon the lipopolysaccharide-induced inflammatory response in human dental pulp cells. *J Cell Mol Med*. 2018;22:2558–68.
24. Statello L, Guo CJ, Chen LL, Huarde M. Gene regulation by long non-coding RNAs and its biological functions. *Nat Rev Mol Cell Biol*. 2021;22:96–118.
25. Park JW, Fu S, Huang B, Xu RH. Alternative splicing in mesenchymal stem cell differentiation. *Stem Cells*. 2020;38:1229–40.
26. Ramos AD, Andersen RE, Liu SJ, Nowakowski TJ, Hong SJ, Gertz C, et al. The long noncoding RNA Pnky regulates neuronal differentiation of embryonic and postnatal neural stem cells. *Cell Stem Cell*. 2015;16:439–47.
27. Aich M, Ansari AH, Ding L, Iesmantavicius V, Paul D, Choudhary C, et al. TOBF1 modulates mouse embryonic stem cell fate through regulating alternative splicing of pluripotency genes. *Cell Rep*. 2023;42: 113177.
28. Peng S, He T, Liu Y, Zheng L, Zhong Y, Niu Z, et al. Lnc-PPP2R1B Mediates the Alternative Splicing of PPP2R1B by Interacting and Stabilizing HNRNPLL and Promotes Osteogenesis of MSCs. *Stem Cell Rev Rep*. 2023;19:1981–93.
29. Chen Z, Zhang K, Qiu W, Luo Y, Pan Y, Li J, et al. Genome-wide identification of long noncoding RNAs and their competing endogenous RNA networks involved in the odontogenic differentiation of human dental pulp stem cells. *Stem Cell Res Ther*. 2020;11:114.
30. Lu Y, Xu W, Ji J, Feng D, Sourbier C, Yang Y, et al. Alternative splicing of the cell fate determinant Numb in hepatocellular carcinoma. *Hepatology*. 2015;62:1122–31.
31. Fagg WS, Liu N, Braunschweig U, Pereira DCK, Chen X, Dittmars FS, et al. Definition of germ layer cell lineage alternative splicing programs reveals a critical role for Quaking in specifying cardiac cell fate. *Nucleic Acids Res*. 2022;50:5313–34.
32. Lokody I. Alternative splicing: Characterizing cell fate. *Nat Rev Genet*. 2014;15:706.
33. Xu Y, Zhao W, Olson SD, Prabhakara KS, Zhou X. Alternative splicing links histone modifications to stem cell fate decision. *Genome Biol*. 2018;19:133.
34. Sun X, Setrerrahmane S, Li C, Hu J, Xu H. Nucleic acid drugs: recent progress and future perspectives. *Signal Transduct Target Ther*. 2024;9:316.
35. Bhaskaran V, Yao Y, Bei F, Peruzzi P. Engineering, delivery, and biological validation of artificial microRNA clusters for gene therapy applications. *Nat Protoc*. 2019;14:3538–53.
36. Khorkova O, Wahlestedt C. Oligonucleotide therapies for disorders of the nervous system. *Nat Biotechnol*. 2017;35:249–63.
37. Liu X, Homma A, Sayadi J, Yang S, Ohashi J, Takumi T. Sequence features associated with the cleavage efficiency of CRISPR/Cas9 system. *Sci Rep*. 2016;6:19675.
38. Chen Y, Li Z, Chen X, Zhang S. Long non-coding RNAs: From disease code to drug role. *Acta Pharm Sin B*. 2021;11:340–54.
39. Liu L, Yang Y, Deng Y, Zhang T. Nanopore long-read-only metagenomics enables complete and high-quality genome reconstruction from mock and complex metagenomes. *Microbiome*. 2022;10:209.
40. Orellana LH, Krüger K, Sidhu C, Amann R. Comparing genomes recovered from time-series metagenomes using long- and short-read sequencing technologies. *Microbiome*. 2023;11:105.
41. Liu M, Jia W, Bai L, Lin Q. Dysregulation of lncRNA TFAP2A-AS1 is involved in the pathogenesis of pulpitis by the regulation of microRNA-32-5p. *Immun Inflamm Dis*. 2024;12: e1312.
42. Yang C, Xu X, Lin P, Luo B, Luo S, Huang H, et al. Overexpression of long noncoding RNA MCM3AP-AS1 promotes osteogenic differentiation of dental pulp stem cells via miR-143-3p/IGFBP5 axis. *Hum Cell*. 2022;35:150–62.
43. Shi Q, Zheng M. Role of LINC01133 in osteogenic differentiation of dental pulp stem cells by targeting miR-199b-5p. *Oral Health Prev Dent*. 2022;20:173–84.
44. Wang J, Liu X, Wang Y, Xin B, Wang W. The role of long noncoding RNA THAP9-AS1 in the osteogenic differentiation of dental pulp stem cells via the miR-652-3p/VEGFA axis. *Eur J Oral Sci*. 2021;129: e12790.
45. Wu Y, Lian K, Sun C. LncRNA LEF1-AS1 promotes osteogenic differentiation of dental pulp stem cells via sponging miR-24-3p. *Mol Cell Biochem*. 2020;475:161–9.
46. Liu Z, Xu S, Dao J, Gan Z, Zeng X. Differential expression of lncRNA/miRNA/mRNA and their related functional networks during the osteogenic/odontogenic differentiation of dental pulp stem cells. *J Cell Physiol*. 2020;235:3350–61.
47. Liao C, Zhou Y, Li M, Xia Y, Peng W. LINC00968 promotes osteogenic differentiation in vitro and bone formation in vivo via regulation of miR-3658/RUNX2. *Differentiation*. 2020;116:1–8.
48. Chen XD, Liu HL, Li S, Hu KB, Wu QY, Liao P, et al. The latest role of nerve-specific splicing factor PTBP1 in the transdifferentiation of glial cells into neurons. *Wiley Interdiscip Rev RNA*. 2023;14: e1740.
49. Zhang B, He W, Pei Z, Guo Q, Wang J, Sun M, et al. Plasma proteins, circulating metabolites mediate causal inference studies on the effect of gut bacteria on the risk of osteoporosis development. *Ageing Res Rev*. 2024;101: 102479.
50. Zhang Y. LncRNA-encoded peptides in cancer. *J Hematol Oncol*. 2024;17:66.
51. Yi Q, Feng J, Lan W, Shi H, Sun W, Sun W. CircRNA and lncRNA-encoded peptide in diseases, an update review. *Mol Cancer*. 2024;23:214.
52. Romero-Barrios N, Legascue MF, Benhamed M, Ariel F, Crespi M. Splicing regulation by long noncoding RNAs. *Nucleic Acids Res*. 2018;46:2169–84.
53. Beltran M, Puig I, Peña C, García JM, Alvarez AB, Peña R, et al. A natural antisense transcript regulates Zeb2/Sip1 gene expression during Snail1-induced epithelial-mesenchymal transition. *Genes Dev*. 2008;22:756–69.
54. Villamizar O, Chambers CB, Riberdy JM, Persons DA, Wilber A. Long non-coding RNA Saf and splicing factor 45 increase soluble Fas and resistance to apoptosis. *Oncotarget*. 2016;7:13810–26.
55. Shaath H, Vishnubalaji R, Elango R, Kardoosha A, Islam Z, Qureshi R, et al. Long non-coding RNA and RNA-binding protein interactions in cancer: Experimental and machine learning approaches. *Semin Cancer Biol*. 2022;86:325–45.
56. Teng L, Feng YC, Guo ST, Wang PL, Qi TF, Yue YM, et al. The pan-cancer lncRNA PLANE regulates an alternative splicing program to promote cancer pathogenesis. *Nat Commun*. 2021;12:3734.
57. Fredericks AM, Cygan KJ, Brown BA, Fairbrother WG. RNA-Binding Proteins: Splicing Factors and Disease. *Biomolecules*. 2015;5:893–909.
58. Fu XD, Ares MJ. Context-dependent control of alternative splicing by RNA-binding proteins. *Nat Rev Genet*. 2014;15:689–701.
59. Wang Z, Rolish ME, Yeo G, Tung V, Mawson M, Burge CB. Systematic identification and analysis of exonic splicing silencers. *Cell*. 2004;119:831–45.
60. Rothrock CR, House AE, Lynch KW. HnRNP L represses exon splicing via a regulated exonic splicing silencer. *Embo J*. 2005;24:2792–802.
61. Wang Z, Xiao X, Van Nostrand E, Burge CB. General and specific functions of exonic splicing silencers in splicing control. *Mol Cell*. 2006;23:61–70.
62. Kashima T, Rao N, David CJ, Manley JL. hnRNP A1 functions with specificity in repression of SMN2 exon 7 splicing. *Hum Mol Genet*. 2007;16:3149–59.
63. Yamazaki T, Liu L, Manley JL. TCF3 mutually exclusive alternative splicing is controlled by long-range cooperative actions between hnRNPH1 and PTBP1. *RNA*. 2019;25:1497–508.

Publisher's Note

Springer Nature remains neutral with regard to jurisdictional claims in published maps and institutional affiliations.